JOURNAL OF MATERIALS SCIENCE 26 (1991) 4399–4406

Effect of yttrium near the interface on reaction and strength of sintered-SiC/Ni couple

Y. IINO
Toyota Technological Institute, Hisakata 2-12, Tempaku, 468 Nagoya, Japan

The effect of yttrium on reaction and bending strength of a pressureless-sintered SiC/Ni couple solid-state bonded in the range 923–1193 K was studied. The reaction between SiC and Ni is retarded by yttrium which was mixed into the SiC and Ni surfaces to a few micrometres depth by electric discharge machining. Si diffusion into Ni is retarded significantly by yttrium, but Ni diffusion into the SiC boundary phase is not. The four-point bending strength of the joined couple at room temperature is slightly improved by the treatment (maximum strength ~110 MPa). Void or coalesced voids were observed at the reaction zone front, where fracture mainly initiated. Yttrium decreases the tendency of void formation. Void formation might be due to an imbalance of interdiffusable amounts between Si in the SiC boundary phase and the Ni bulk.

1. Introduction

The reaction of hot-pressed or single-crystal SiC/Ni takes place at comparatively low temperatures (above ~ 950 K) forming reaction zones where silicides, Ni_2Si, Ni_3Si_2, etc., are found [1–3]. In the case of a sintered SiC/Ni couple, a more significant reaction would take place, because the SiC contains a boundary phase. In the joining of sintered SiC to Ni, Yamada *et al.* [4] reported the formation of a large reaction zone where Ni_5Si_2 was formed. They did not, however, evaluate the bond strength.

When a joined couple is to be used for high-temperature application, retardation of the reaction is necessary. Alloying elements Cr and Cr + Al act to retard the reaction, mainly by forming carbide and a complex metal reaction product which are barriers to diffusion of Ni to hot-pressed SiC [1].

Another method of producing a barrier might be the use of an element which has very large atomic diameter compared with Ni (2.5×10^{-10} m diameter) and Si (2.34×10^{-10} m diameter). According to the Hume–Rothery 15% rule, an element with a 15% larger atomic diameter than these elements could not make a solid solution with them. Yttrium (3.65×10^{-10} m diameter) is one such element. Mixing or implantation of yttrium into the Ni surface has been done successfully by electric discharge machining, by which yttrium is transfered into the Ni surface to a few micrometres depth [5].

In this study, joining of sintered SiC to Ni with and without surface treatment by electric discharge machining was carried out. The effect of yttrium on reaction-zone formation was examined metallographically. The four-point bending strength was also evaluated.

2. Materials and specimen preparation

Pressureless-sintered 97% SiC used in the present study contained C, SiO_2, B, Al and small amounts of other metallic elements. The microstructure etched in alkali solution is shown in Fig. 1a. It consists of SiC grains and a continuous boundary phase. It was supplied in the form of a block (12 mm × 14 mm × 35 mm), which was cut into two parts at mid-length (12 mm × 14 mm × 17 mm). The cut surfaces were polished with 9 μm diamond polishing film and were used as bonding surfaces. The Ni used was 99.9 wt % purity and in the form of a sheet (1 mm × 100 mm × 100 mm), from which pieces of 1 mm × 12 mm × 14 mm were cut.

Bonding surface of SiC and two bonding surfaces of Ni were electric discharge machined in kerosene with a 99.9 wt % yttrium electrode (15 mm × 15 mm × 15 mm). The machining conditions are given in Table I. The machining time was about 1 h. Fig. 1b–e show the microstructure of the machined surface of SiC and the yttrium distribution. The microstructure and distribution of Ni are given in [5]. SiC and Ni with machined surfaces are termed SiC(Y) or (Y)SiC and (Y)Ni or Ni(Y), respectively. The materials were cleaned ultrasonically in acetone immediately prior to joining.

Sandwich-like bonding couples, SiC(Y)/(Y)Ni(Y)/(Y)SiC and SiC/Ni/SiC (a couple without electric discharge machining) were joined in a vacuum chamber installed with an induction heating coil and an axial loading rod. The specimens were heated using a Mo susceptor heated by the high-frequency heating apparatus. The bonding conditions were a vacuum, V_{ac}, of ~ 10^{-4} Pa, a bonding temperature, T, of 923–1193 K, a bonding compressive stress, S, of 20 MPa, and a bonding time, t, of 2.7–21.6 ks. The heating rate to bonding temperature was 0.4 K s^{-1} and the cooling rate was 0.4 K s^{-1} to ~ 700 K, followed by furnace cooling.

From the joined couple, four-point bending

0022–2461/91 $03.00 + .12

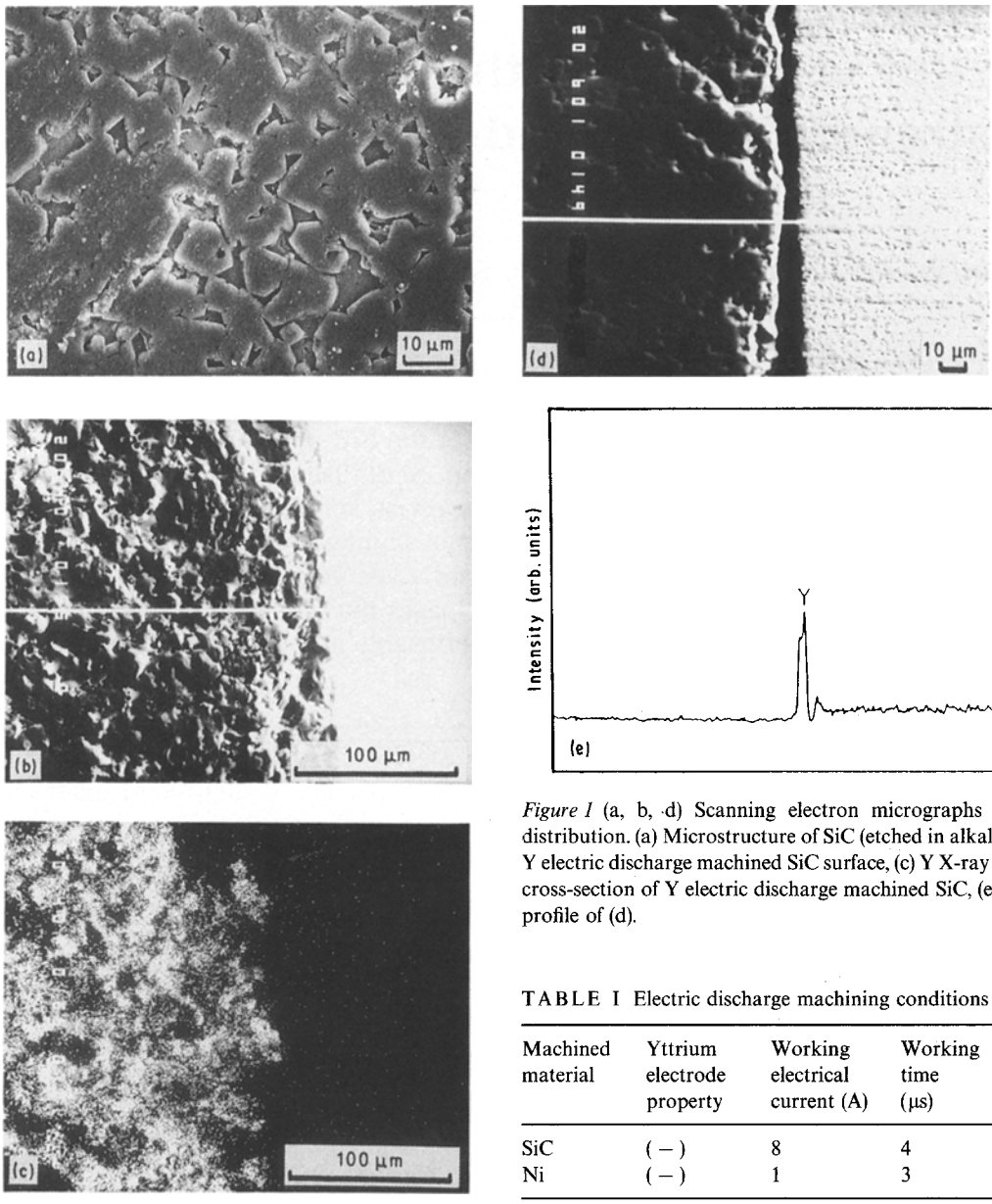

Figure 1 (a, b, d) Scanning electron micrographs and (c, e) Y distribution. (a) Microstructure of SiC (etched in alkali solution), (b) Y electric discharge machined SiC surface, (c) Y X-ray map of (b), (d) cross-section of Y electric discharge machined SiC, (e) Y X-ray line profile of (d).

TABLE I Electric discharge machining conditions

Machined material	Yttrium electrode property	Working electrical current (A)	Working time (μs)	Resting time (μs)
SiC	(−)	8	4	1024
Ni	(−)	1	3	2

specimens, 4 mm × 3 mm × 35 mm, were machined. Surfaces of the specimens were polished using 3 μm diamond polishing film and the edges were bevelled to remove flaws that might cause premature failure. The four-point bending test was done at room temperature using an Instron-type testing machine at a crosshead speed of 0.5 mm min^{-1}. The bending strength was calculated using the fracture load. The fracture surface was observed using a scanning electron microscope (SEM) and the element distribution across the interface was examined by electron probe microanalysis (EPMA).

3. Results

3.1. Reaction zones

In both couples, reaction zones were found as illustrated in Figs 2a, 3a and 4a. The zone thickness increases with increasing bonding time and bonding temperature. The reaction zone thickness in SiC, R_{SiC}, and that in Ni, R_{Ni}, schematically shown in Fig. 5 (I is not the initial SiC/Ni or SiC(Y)/(Y)Ni interface but an apparent interface) were measured by either optical microscopy or SEM; they are given in Table II. From the data, it is seen (1) that R_{Ni} in the SiC/Ni couple is larger than R_{SiC} except at $T = 923$ K, while R_{Ni} in SiC(Y)/(Y)Ni couple is very small compared with R_{SiC} (see ratio of R_{Ni} to R_{SiC}), and (2) that R_{Ni} in SiC(Y)/(Y)Ni is smaller than SiC/Ni for a given bonding condition (compare R_{Ni} at $T = 1193$ K and $t = 5.4$ ks of SiC/Ni with SiC(Y)/(Y)Ni). The effect of yttrium near the interface on the reaction was found to be significant.

Fig. 6 shows the relation between R_{Ni} zone thickness and the square root of bonding time of SiC(Y)/(Y)Ni at two bonding temperatures. The linear relation after an incubation time indicates that the reaction is diffusion controlled. The incubation time for R_{Ni} formation, i.e. time at zero reaction zone thickness extrapolated by the lines, increases with decreasing bonding temperature.

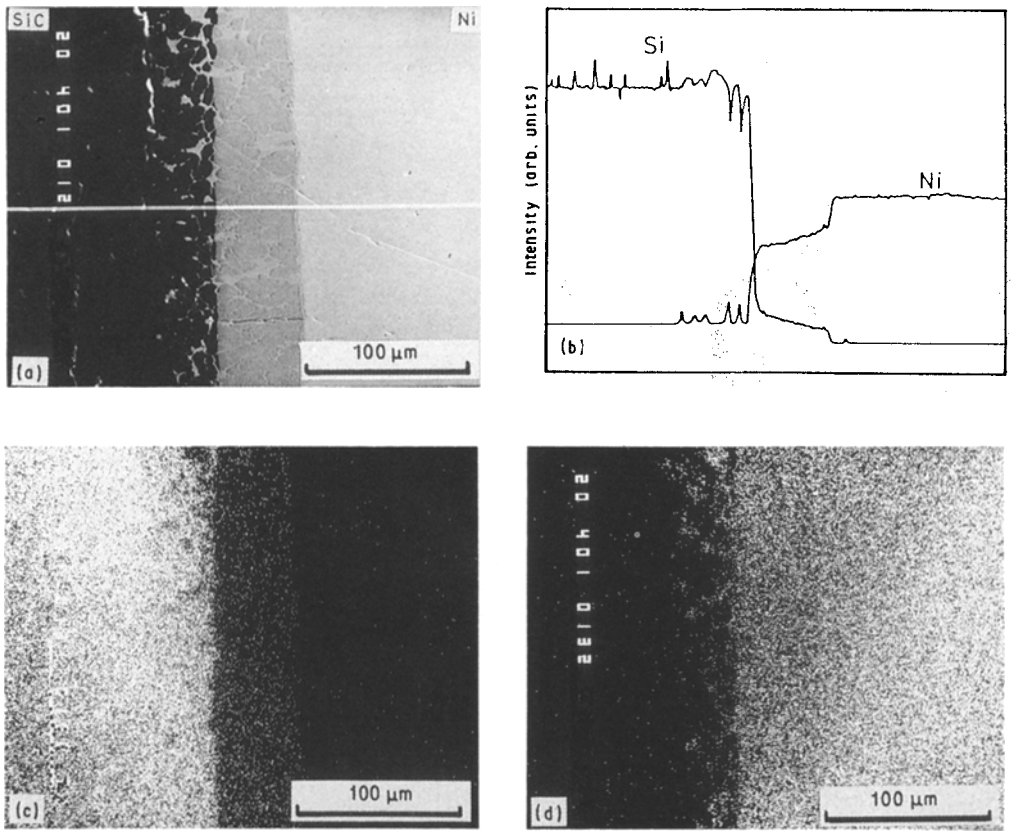

Figure 2 X-ray map of SiC/Ni couple bonded at 1123 K for 5.4 ks. (a) Secondary electron image, (b) line profile, (c) Si X-ray map, (d) Ni X-ray map.

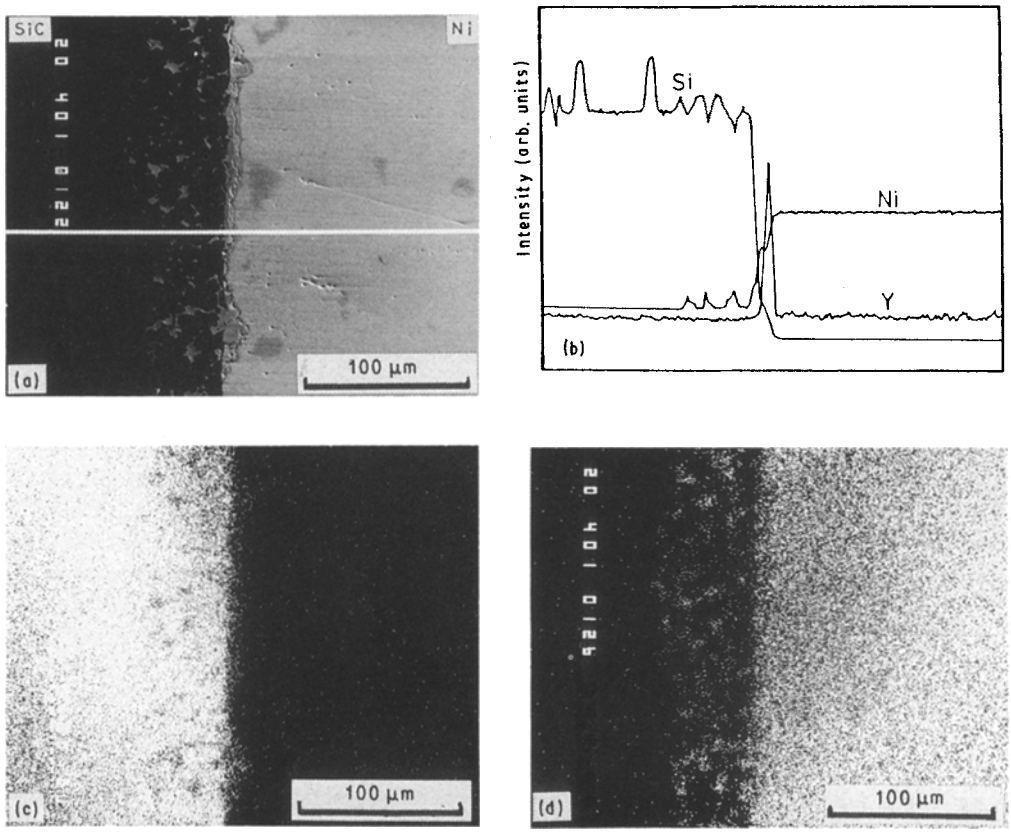

Figure 3 X-ray map of SiC(Y)/(Y)Ni couple bonded at 1123 K for 5.4 ks. (a) Secondary electron image, (b) line profile, (c) Si X-ray map, (d) Ni X-ray map, (e) Y X-ray map.

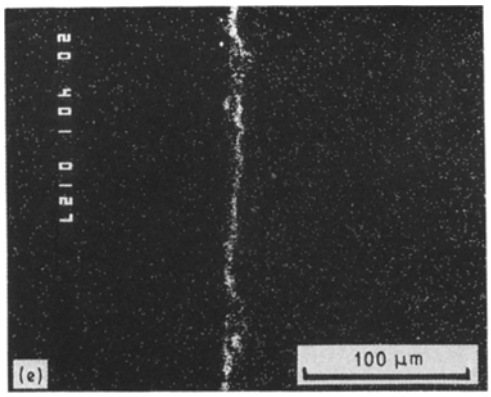

Figure 3 Continued.

In the SiC(Y)/(Y)Ni couple, they are formed at the Ni side below $t = 5.4$ ks and at the SiC side above $t = 10.8$ ks. Voids in SiC side increased with increasing bonding temperature and bonding time.

3.3. Four-point bending strength

SiC/Ni couples bonded at 1193 and 1273 K fractured during machining of the bend specimen. This was found to be caused by coalesced voids at the R_{SiC} zone front. Thus the strength of these specimens was assumed to be 0. Bonding-temperature dependence of four-point bending strength, σ, for $t = 5.4$ ks is shown in Fig. 8. The maximum strength of SiC/Ni was at 1023 K, while that of SiC(Y)/(Y)Ni increased up to $\sim$ 1200 K. This means that SiC/Ni couple becomes more heat-resistant with yttrium near the interface.

The effect of bonding time on σ of SiC(Y)/(Y)Ni is shown in Fig. 9, where three sets of SiC/Ni data are also plotted for $t = 73.5\ s^{1/2}$ (5.4 ks). At 1123 K, σ is almost the same for $t = 73.5\ s^{1/2}$ and $103.9\ s^{1/2}$ (10.8 ks). At 1193 K, it decreases significantly above $t = 103.9\ s^{1/2}$. The decrease was found to be due to the formation of many voids at the R_{SiC} zone front, where the fracture initiated (the fracture initiation site is shown in Table II). By comparison of the fracture initiation site and the strength, it is seen that when

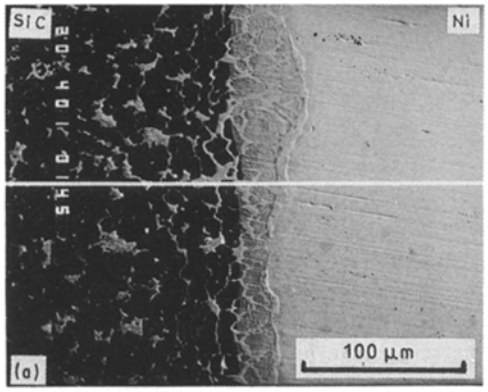

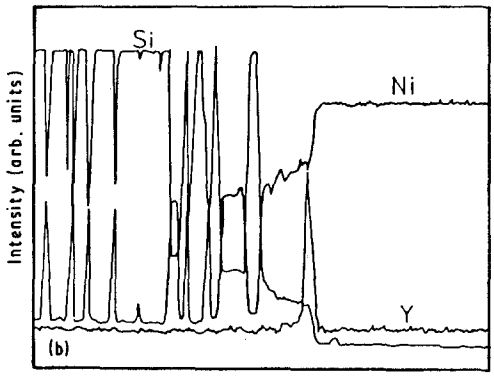

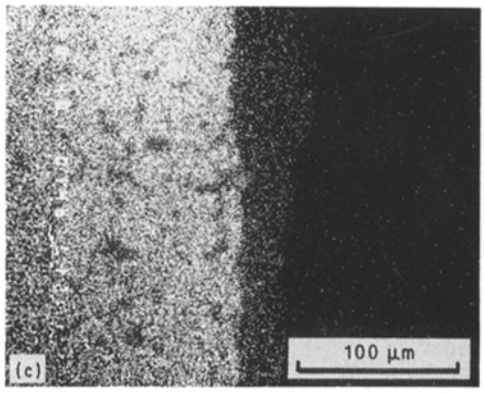

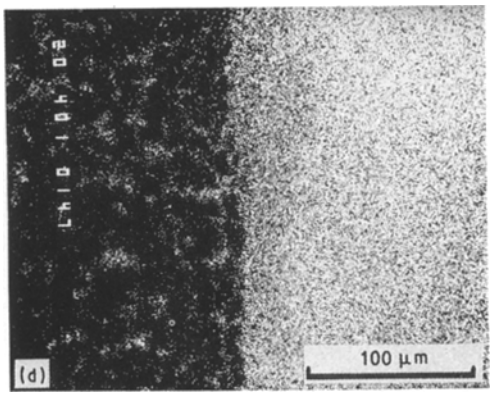

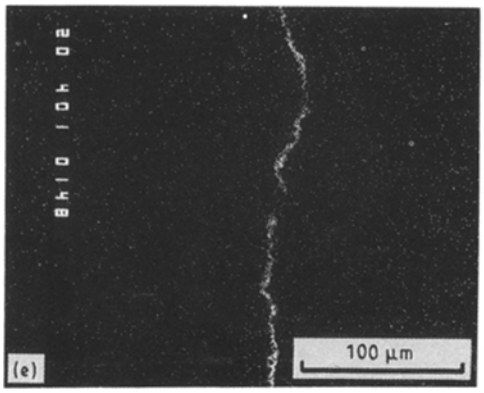

Figure 4 X-ray map of SiC(Y)/(Y)Ni couple bonded at 1123 K for 10.8 ks. (a) Secondary electron image, (b) line profile, (c) Si X-ray map, (d) Ni X-ray map, (e) Y X-ray map.

3.2. Void or microcrack formation

Voids and microcracks are observed at the reaction zone fronts by SEM, and are illustrated in Fig. 7. Observed voids or microcracks are marked V (void) or C (microcrack) in Table II. In the SiC/Ni couple, voids are formed only at the SiC side, i.e. at R_{SiC} zone front.

TABLE II Reaction zone thickness and fracture initiation sites

Couple	Bonding temperature (K)	Bonding time (ks)	Reaction zone thickness[a]		R_{Ni}/R_{SiC}	Fracture initiation site of four specimens				
			R_{SiC} (μm)	R_{Ni} (μm)		SiC	R_{SiC} front	I	R_{Ni} front	Ni
SiC/Ni	923	5.4	10	2	0.2		....			
	1023	5.4	15 V (fine)	22	1.47		....			
	1123	5.4	38 V (large)	50	1.32		....			
	1193	5.4		108			....[b]			
	1273	5.4	104 V (large), C	172	1.65		....[b]			
SiC(Y)/	1123	5.4	50	4 V (few), C	0.08			..	..	
(Y)Ni	1123	10.8	150 V (fine)	29	0.19	..			..	
	1193	2.7	90 V (few)	28 C	0.31	..			..	
	1193	5.4	130 V (fine)	31 V (fine), C	0.24			.	...	
	1193	10.8	250 V (large)	85	0.34		....			
	1193	21.6	340 V (large)	162	0.48		....			

[a] V = void, C = microcrack observed at reaction zone front on scanning electron micrograph of ×1000. Few, few fine void; fine, fine void; large, large coalesced void.
[b] Fractured during machining bending specimen.

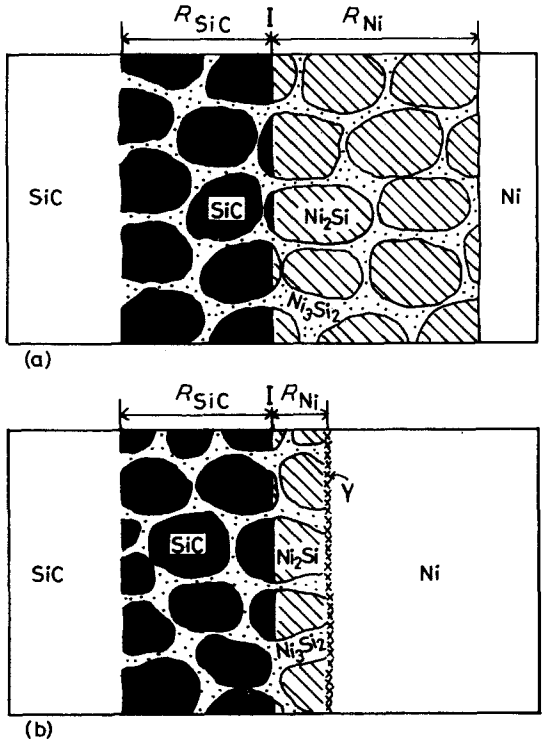

Figure 5 Schematic drawing of reaction zones, reaction zone thickness (R_{SiC} and R_{Ni}) and main reaction products of (a) SiC/Ni and (b) SiC(Y)/(Y)Ni couple. R_{SiC} is the distance from the apparent interface, I, to the SiC reaction zone front; R_{Ni} is the distance from I to the Ni reaction zone front.

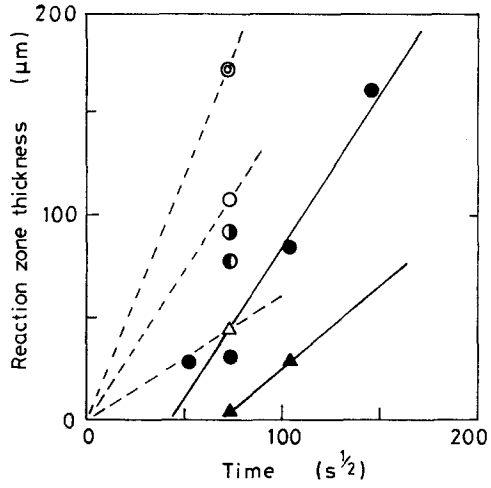

Figure 6 Reaction zone thickness, R_{Ni}, versus square root of bonding time. SiC/Ni: (△) 1123 K, (○) 1193 K, (◎) 1273 K; SiC/(Y)Ni: (◑) 1193 K; SiC(Y)/Ni: (◐) 1193 K; SiC(Y)/(Y)Ni: (▲) 1123 K, (●) 1193 K.

many voids or coalesced voids are formed at the R_{SiC} zone front, fracture initiates there and the strength decreases significantly.

3.4. Element distribution

The results of Si, Ni and Y analysis by EPMA across the reaction zones in Figs 2–4a are shown in Figs 2b–d, 3b–e and 4b–e. In the R_{SiC} zone, Ni is detected only on the boundary phase (grey nett-like region), and Si intensively on the SiC grains (black island-like area). Yttrium is detected at the R_{Ni} zone front; Si diffusion front. It is not diffused away but concentrated at the Si-diffusion front even at high temperatures and long bonding times (1193 K, 10.8 ks).

Because R_{Ni} in SiC(Y)/(Y)Ni is very small compared with that of SiC/Ni (Table II), it is thought that yttrium acts as barrier to Si-diffusion into Ni. However, it does not act as a barrier to Ni diffusion into the boundary phase of SiC; note the rather larger R_{SiC} of SiC(Y)/(Y)Ni (50 μm) than that of SiC/Ni (30 μm) at 1123 K for 5.4 ks (Table II).

4. Discussion

4.1. Reaction zone

When a reaction is diffusion controlled, the relation between reaction zone thickness and square root of time is expressed by a line which is extrapolated to the origin of the plot [1, 5]. Assuming that the present SiC/Ni reaction is also diffusion controlled, dotted lines are drawn in Fig. 6. By plotting the logarithm of the rate of reaction zone formation (in $\mu m^2 s^{-1}$) versus

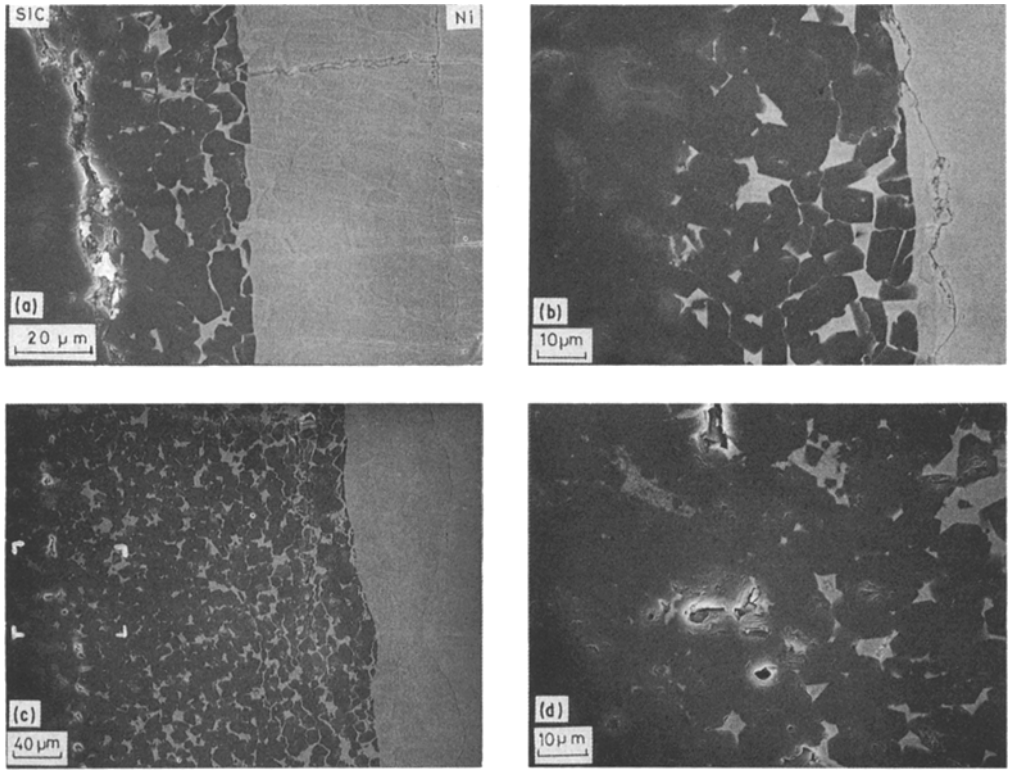

Figure 7 Void, coalesced void or microcrack at reaction zone fronts (scanning electron micrographs). (a) SiC/Ni couple bonded at 1123 K for 5.4 ks, (b) SiC(Y)/(Y)Ni couple bonded at 1123 K for 5.4 ks, (c) SiC(Y)/(Y)Ni couple bonded at 1193 K for 10.8 ks, (d) enlarged view of the area marked in (c).

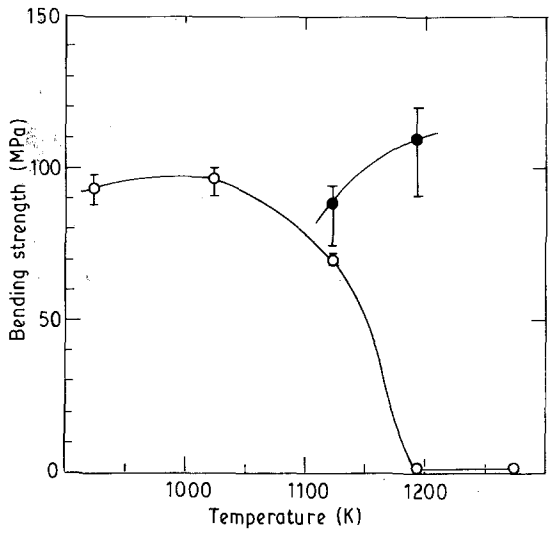

Figure 8 Four-point bending strength at room temperature versus bonding temperature, for (○) SiC/Ni, (●) SiC(Y)/(Y)Ni. Bonding time 5.4 ks. I , scatter of strength of four specimens; (○, ●) mean value.

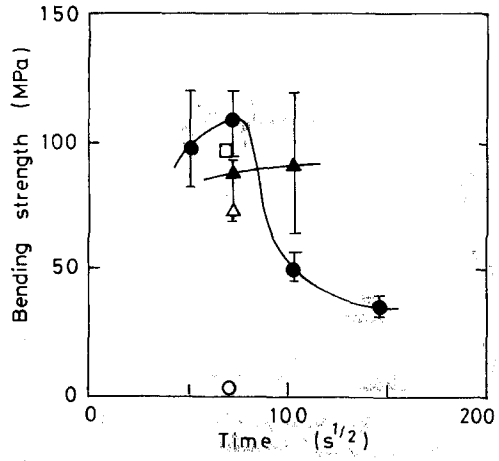

Figure 9 Four-point bending strength at room temperature versus square root of bonding time. SiC/Ni: (□) 1023 K, (△) 1123 K, (○) 1193 K; SiC(Y)/(Y)Ni: (▲) 1123 K, (●) 1193 K.

the reciprocal of the absolute temperature, the apparent activation energy for the process can be calculated. The Arrhenius plot is shown in Fig. 10. The activation energy, Q, was calculated to be 183 kJ mol^{-1}. Yamada *et al.*'s results (Fig. 7 of [4]) are replotted in Fig. 10. The activation energy of the present work agrees well with their results (180.5 kJ mol^{-1}).

The linear relation between reaction zone thickness and square root of time for SiC(Y)/(Y)Ni after the incubation time (solid lines in Fig. 6) also indicates that the reaction is diffusion-controlled. The Arrhenius plot is shown in Fig. 10. Although there are only two experimental data, Q was calculated to be 191 kJ mol^{-1}, which is somewhat larger than SiC/Ni.

The incubation time in the case of the SiC(Y)/(Y)Ni couple, would be caused by (1) the rough surfaces produced by electric discharge machining, and (2) yttrium near the interface. At the beginning of the bonding, the rough (Y)Ni(Y) surface is deformed to contact with the rough (Y)SiC surface, then yttrium in the SiC surface is pushed into the Ni interface and begins to move, together with the yttrium in the Ni surface, into the Ni bulk. This period is termed the incubation time. The effect of surface roughness of

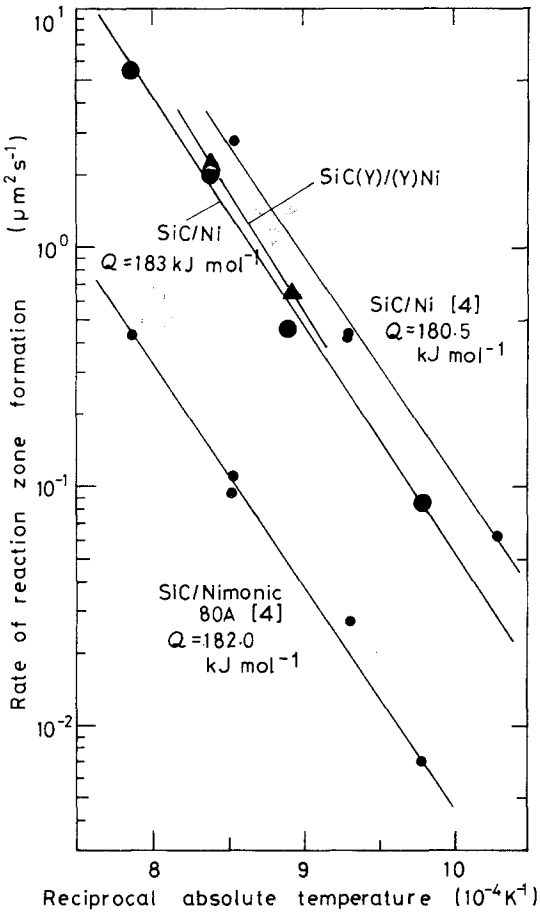

Figure 10 Rate of nickel reaction zone (R_{Ni}) formation versus reciprocal of absolute temperature. (▲) Arrhenius plot.

(Y)Ni on the incubation time would, however, be small, because at bonding temperatures of 1123 and 1193 K and under a bonding pressure of 20 MPa, the rough Ni surface would deform soon after the beginning of bonding. The incubation time depends on where yttrium is situated; as seen in Fig. 6, R_{Ni} thickness at 1193 K for 5.4 ks is 108 μm for the SiC/Ni couple, 93 μm for the SiC/(Y)Ni couple, 76 μm for the SiC(Y)/Ni and 31 μm for the SiC(Y)/(Y)Ni.

According to the Hume–Rothery 15% rule, two elements with a difference in size larger than 15%, makes less solid solution. So yttrium in the present experiment diffuses little in Ni but is concentrated at the R_{Ni} zone front. The reason why yttrium does not diffuse into the SiC boundary phase but does into Ni is not known. One possible cause might be that the difference in atomic size is larger in the case between Si and Y than Ni and Y, and there might be many complex compounds in the boundary phase of SiC material.

X-ray diffraction analysis of reaction zones (R_{SiC} and R_{Ni}) were done on the SiC/Ni couple bonded at 1273 K for 5.4 ks, where very thick reaction zones were formed, making the analysis convenient. SiC and Ni_3Si_2 were detected in the SiC reaction zone and Ni_3Si_2 and Ni_2Si in the Ni reaction zone. Other elements, C, B, Al, and other compounds, would also exist in the zones.

Taking into account the microstructural features shown in Figs 2–4, the element distribution across the interface and X-ray analysis, the reaction zone is schematically drawn in Fig. 5. In R_{SiC}, not only a boundary phase but also a grain boundary of SiC grains would have reacted with Ni that has diffused into the boundary phase, forming Si, N, Ni_3Si_2 and other products (compare the angular SiC grain in Fig. 1a with the somewhat rounded SiC grain and the larger boundary-phase area in Fig. 7). In R_{Ni}, Si reacts with Ni to form Ni_3Si_2 and Ni_2Si.

4.2. Void formation

Voids are found at reaction zone fronts. The formation might be due to the imbalance of interdiffusable amounts between Si and Ni. In the case of the SiC/Ni couple, Si in R_{SiC} diffuses through a continuous boundary phase and the interface into Ni. The diffusable amount of Si in R_{SiC} is not enough (the volume of the boundary phase is very small compared with that of Ni). The supply of Si from the boundary phase in non-reacted SiC bulk and that from the SiC grain in R_{SiC} formed by the reaction of the SiC grain and Ni is not enough. So an insufficiency of Si at the R_{SiC} front occurs. Accordingly, a void is formed at the zone front. The Ni content is sufficient for diffusion through the interface into the boundary phase in SiC, and no void is formed at the R_{Ni} zone front.

In the case of the SiC (Y)/(Y)Ni couple, the diffusion process is not simple because of yttrium, which acts as a diffusion barrier and yet moves, although slowly, into Ni with bonding time. When the bonding time is short, Ni in R_{Ni} (very thin at short times) diffuses into the SiC boundary phase very rapidly because of the steep concentration gradient of Ni. But the supply of Ni from the matrix is not enough due to the yttrium concentration at the R_{Ni} zone front. The diffusable amount of Ni in R_{Ni} is not enough and an insufficiency of Ni in the R_{Ni} zone front occurs. This causes void formation at the R_{Ni} zone front and microcracks would be initiated during cooling to room temperature.

With increasing bonding time, R_{Ni} increases. Although the R_{Ni} thickness is smaller than R_{SiC}, the volume of R_{Ni} and that of the boundary phase in R_{SiC} would become comparable. Balanced interdiffusion between Si and Ni can occur and no void, or only a very tiny void, is formed both at the R_{SiC} and R_{Ni} zone fronts.

With further increasing bonding time, the R_{Ni} thickness increases. Si in R_{SiC} becomes insufficient, as in the case of SiC/Ni. This causes void formation and coalescence at the R_{SiC} zone front.

As shown in Table II, fracture occurs mainly at voids or the microcrack-formed reaction zone front. In these cases, the fracture strength is reduced.

5. Conclusions

1. Yttrium can be mixed into the SiC surface by electric discharge machining.

2. In both SiC/Ni and SiC(Y)/(Y)Ni couples, SiC and Ni reaction zones are formed. Ni diffuses into the boundary phase of SiC to form Ni_3Si_2 and Si into Ni to form Ni_3Si_2 and Ni_2Si.

3. Yttrium near the interface acts as a diffusion barrier to Si, but not to Ni. The Ni reaction zone is greatly reduced by yttrium.

4. Fracture strength is slightly improved by yttrium electric discharge machining of the surface to be bonded.

5. In the SiC/Ni couple, a void is formed at the SiC reaction zone front. This might be due to an imbalance of the amounts of diffusable Si and Ni. Fracture begins at the reaction zone front. The bending strength decreases significantly when void coalescence takes place.

6. In the SiC(Y)/(Y)Ni couple, the void formation site changes with bonding time; first at the Ni reaction zone front, then no observable voids at both zone fronts, and finally at the SiC reaction zone front as in SiC/Ni.

Acknowledgement

The author thanks Mr Taguchi for his assistance in the experiments.

References

1. M. R. JACKSON, R. L. MEHAN, A. M. DAVIS and E. L. HALL, *Metall. Trans.* **14A** (1983) 355.
2. M. SAKAI and K. WATANABE, *J. Mater. Sci.* **19** (1984) 3430.
3. S. K. CHOI, L. FROYEN and M. J. BRABERS, "Joining ceramics, glass and metal" (Informationsgesellschaft Verlag,
4. T. YAMADA, H. SEKIGUCHI, H. OKAMOTO, S. AZUMA and A. KITAMURA, "Ceramic materials and components for engines" (Deutsche Keramische Gesellschaft, Lübeck-Travemünde, 1986) p. 441.
5. Y. IINO, T. TAKAMORI, N. MOHRI, N. SAITO and M. SUZUKI, *J. Mater. Sci. Lett.* **8** (1989) 493.

Received 21 March
and accepted 20 December 1990